Control Design of Grid-Connected PV Systems for Power Factor Correction in Distribution Power Systems Using PSCAD

Haider Muaelou, Khaled M. Abo-Al-Ez, and Ebrhim A. Badran
Faculty of Engineering, Mansura University

Abstract: In modern electric power systems, the dependence on solar power is increasing. The grid connected applications are very important with deficit in conventional power stations due to fuel shortage. The design of the control strategy to connect photovoltaic (PV) systems to the electric distribution grid is a challenging issue.

This paper focuses on a controller design and its implementation in grid connected PV systems for power factor correction in distribution power systems. The first step is modeling of the components of the PV system, mainly; the PV source, the DC-DC converter, and the grid interface inverter with the appropriate filter. PSCAD is used for simulating this study. The proposed controller is then designed. The proposed control strategy targets the design of the Maximum Power Point Tracking (MPPT) algorithm, and the control of injected active and reactive power. The control of the reactive power is addressed in this paper to equip the PV system with power factor correction capability, which improves the overall performance at the point of common coupling (PCC). Proposed operation scenarios are suggested to test the controller validity. The results show that the model is accepted and the proposed controller gives the required performance.

Keywords: Control System, PV, Renewable Energy, PFC, DistributionSystem, PSCAD

1. Introduction

Most of the loads in distribution network tend to inductive loads such as induction motor. Those loads need two types of power; active power for the purpose work performing such as motion and reactive power for providing a magnetic field. Those loads absorb the reactive power from the network, reduce the power factor of the network and cause many economiclosses. Therefore, devices for power factor correction must used such as Flexible AC Transmission System (FACTS) devices, Static Var Compensator (SVC) and Static Synchronous Compensator (STATCOM). Availability of sunlight over large areas of the earth's surface encourages growth of many electrical applications of PV systems. So, the solar energy will be a promising source for electric power generation due to fuel shortage [1]. In recent years, much more efforts have been made on the integration of PV systems into the grid in order to meet the imperative demand of a clean and reliable electricity generation. Electric power generation through solar energy process is one of the more methods available at the moment, during the operation of solar energy systems do not generate any greenhouse gas pollution of the environment [2]. This paper presents control strategy of PV systems for the purpose of power factor correction to prevent the instability of the grid voltage for the point of common coupling (PCC).

This paper organized as follows: Section II presents the PV grid-tied system model, the PV solar system model and the proposed control are simulated using PSCAD/EMTDC. Section III describes the validation of the proposed controller at different cases; and Section IV gives the conclusions drawn from this research.

2. PV GRID-TIED SYSTEM MODEL

The solar cell is a semiconductor device that converts the solar radiation directly to electrical energy, with no pollutant emission. The output from a single cell is not suitable for practical cases. To obtain sufficient voltage the cells are connected in series. To obtain sufficient current, they are connected in parallel to form a PV module. The modules can be also connected in series and in parallel to form a PV array with the required rated power [3]. The PV grid-tied model is constructed in PSCAD including PV source, a DC-link capacitor, a DC-DC converter, a DC-DC controller with maximum power point tracking (MPPT), the grid interface inverter with the appropriate filter and step up transformer, as shown in Fig. 1.

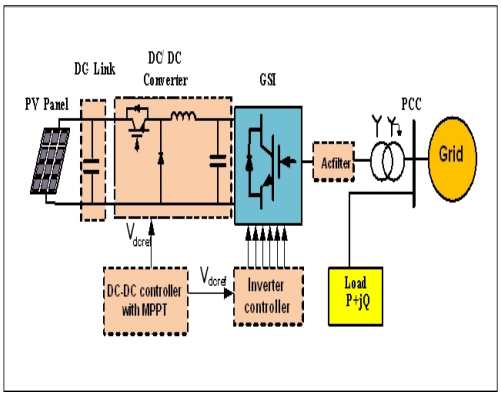

Fig. 1. PV Grid-Tied Construction.

A. PV Source Model

The equivalent electrical circuit of a PV cell which contains a current source anti-parallel with a diode, a shunt resistance, and a series resistance is shown in Fig. 2 [4].

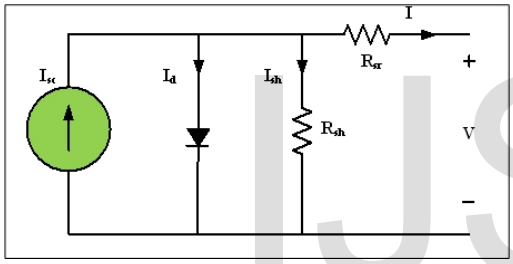

Fig. 2.PV cell equivalent circuit.

The basic equation that characterizes the solar cell I/V relationship can be derived after apply Kirchhoff's current law on PV cell equivalent circuit as;

$$I = I_{sc} - I_d - I_{sh} \qquad (1)$$

I is output cell current, I_{sc} is the short circuit current, I_d is the diode current and I_{sh} is the parallel brance current.

$$I_d = I_o\left[\exp\left(\frac{V+IR_{sr}}{nkT_c/q}\right) - 1\right] \qquad (2)$$

$$I_{sh} = \frac{V+IR_{sr}}{R_{sh}} \qquad (3)$$

After compensation the equation (2) and equation (3) in equation (1) becomes the following equation [2];

$$I = I_{sc} - I_o\left[\exp\left(\frac{V+IR_{sr}}{nkT_c/q}\right) - 1\right] - \left(\frac{V+IR_{sr}}{R_{sh}}\right) \qquad (4)$$

I_{sc} is a function of the solar radiation on the plane of the solar cell G and the cell temperature T_c, as given by [2];

$$I_{sc} = I_{scR}\frac{G}{G_R}[1 + \alpha_T(T_c - T_{cR})] \qquad (5)$$

The current I_o in equation (4) is called the dark current. It is a function of cell temperature only, and is given by [2];

$$I_o = I_{oR}\left(\frac{T_c^3}{T_{cR}^3}\right)\exp\left[\left(\frac{1}{T_{cR}} - \frac{1}{T_c}\right)\frac{qe_g}{nk}\right] \qquad (6)$$

where I_{scR} is the short circuit current at the reference solar radiation G_R and the reference cell temperature T_{cR} . The parameter αT is the temperature coefficient of photo current, I_{oR} is the dark current at the reference temperature, q is the electron charge, k is the Boltzmann constant, e_g is the bandgap energy of the solar cell material, and n is the diode ideality factor. The constants of the above equations are set by the manufacturers.

B. DC Link Capacitor

This element is of great importance as it provides several functions. It minimizes the voltage ripple across the PV terminals which results in a ripple of the output power [3]. The capacitor is the source for reactive power generation. The size of the DC link capacitor can be determined as follows [5];

$$C = \frac{(2P_{max})}{[fV_{dc}^2(1-k^2)]}\ F \qquad (7)$$

where P_{max} is the maximum output power from the PV array, f is the frequency, V_{DC} is the DC-link voltage and K is the ripple factor. For the model used in this paper, shown in Fig. 1, P_{max}≈ 160 kW, f =60 Hz, V_{DC}=500 V and K = 0.02. Then the value of the DC link capacitor is found to be 21350 µF.

C. DC -DC Converter

It is known that the efficiency of the solar PV module is low (about 13%) [6]. So, it is desirable to operate the module at the peak power point in order to maximize the delivered power to the load under varying temperature and solar radiation conditions. Hence, maximization of power improves the utilization of the solar PV module. The dc-dc converter serves the purpose of transferring maximum power from the PV module to the load by changing the duty cycle. The load impedance as seen by the source is varied and matched at the point of the peak power with the source [7]. So, the maximum power is transferred. The available dc-dc converters are step down converter, step up converter and step up-step down converter. In this paper, the buck converter is selectedin order to use a battery with low voltage to provide power continuity at the day night. The converter is used to reduce input voltage when the output requires a lower voltage. It consists of a power switch that is followed by an inductor, a diode and output capacitance, as shown in Fig. 3.

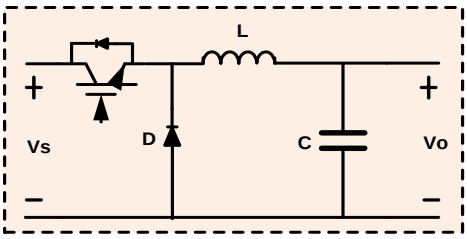

Fig. 3. DC -DC Step down converter model.

The voltage across the inductor when the switch of converter is closed is given by;

$$V_o = \frac{1}{T}\int_0^{t_1} V dt = \frac{t_1}{T} V_S = f t_1 V_S = D V_S \qquad (8)$$

where D $= \frac{t_{on}}{T} = t_{on} \times f$ is the duty cycle of chopper, T is the chopping period (t_{on}+t_{off}), and f is the chopping frequency.

D. DC-DC Converter Controller as a (MPPT)

The relationship between current and voltage of the PV cell is non-linear. I/V curve of the solar cell is shown in Fig. 4. There is an unrivaled point on the I/V curve, called the Maximum Power Point (MPP), at which the entire PV system operates with maximum efficiency and gives its maximum output power. The location of the MPP is not known, but it can be determined, either through calculation models or by search algorithms in order to maintain the PV array's operating point at its MPP.

The optimum operating point of solar cells occurs at the knee of the I/V curve.In this paper the incremental conductance algorithm is used. This method tracks the peak power under fast varying atmospheric condition. In this method the derivative of PV output power with respect to its output voltage is calculated (dP/dV). When dP/dV approaches zero the maximum PV output power can be achieved [8]. The controller calculates dP/dV based on the measured PV incremental output power and voltage. If dP/dV is not close to zero, the controller will adjust the PV voltage step by step until dP/dV approaches zero, at which the PV array reaches its maximum output.

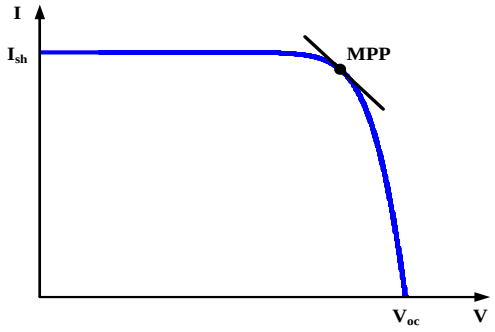

Fig. 4.Typical I/V Characteristics of a PV Cell.

The mathematical description of this method is illustrated using;

$$P = V I \qquad (9)$$

With incremental change in current and voltage, the modified power is given by [9];

$$P+\Delta P = (I+\Delta I).(V+\Delta V) \qquad (10)$$

After ignoring small terms in equation (10) the equation simplified to;

$$\Delta P = \Delta V.I + \Delta I.V \qquad (11)$$

ΔP must be zero at peak point. Therefore, at peak point equation (11) becomes;

$$dI/dV = - I/V \qquad (12)$$

The incremental algorithm based on the following equation holds at the MPP is [8]:

$$dI/dV + (I/V) = 0 \qquad (13)$$

Theflow chart which describes the detailed operations of theincremental algorithm is shown in Fig. 5 [10].

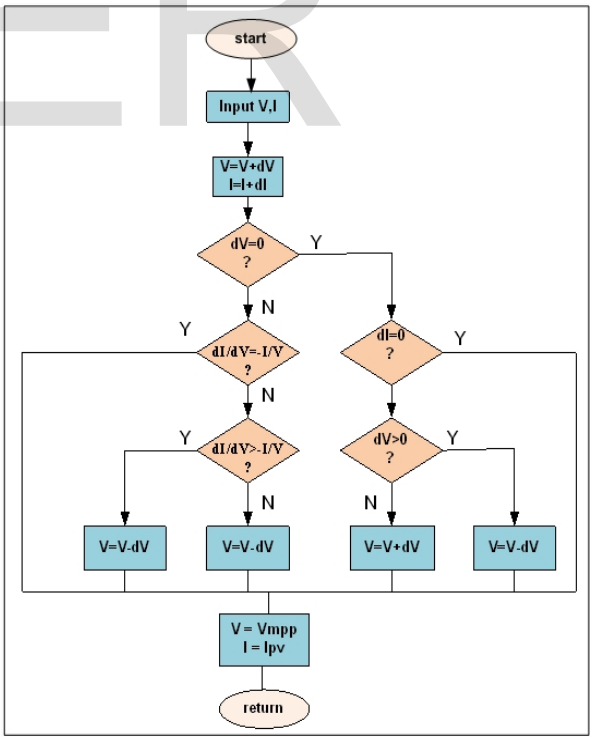

Fig. 5.Flow chart of the incremental MPP algorithm [10]

E. DC-DC Converter Controller Model

The objective of the converter control is to keep the PV voltage (Vpv) at value equals to the voltage (Vmppt) at MPPT. The voltage output the PV system and the reference voltage is compared, using this difference as an enter to the Proportional Integral (PI) controller to produce the so-called duty cycle. The duty cycle is defined as the small part of the stage through which the switch is onranges between 0 and 1. If the duty cycle is equale to 0.5 that means the switch is equal in both time on and off. If the value larger than 0.5 the on time of the switch is bigger, if the of duty cycle is fewer than 0.5 that means off time of the switch is bigger [11]. The pulse width modulation (PWM) signal T1 was produced through compared the signal of the duty cycle with a triangler signal with magnitude between 0 to 1, as shown in Fig. 6. The comparator is setting to generate 1 at what time the duty cycle is larger than the triangle signal and generate 0 otherwise creating pulses with a magnitude of 1 and with pulse widths which depend on the duty cycle.

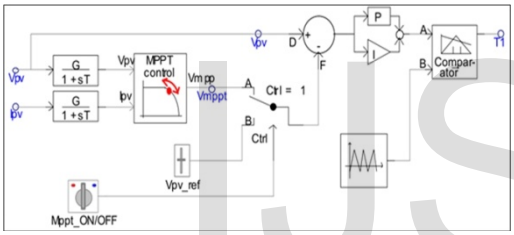

Fig. 6. D.C-to-D.C Converter Controllermodel inPSCAD.

F. DC-AC Switch Mode Inverters

The conversion of DC output power of the PV system to athree phase AC power is performed using the three phaseDC-AC inverter. Switch mode inverters produce a sinusoidal AC outputfrom a DC input through PWM. The inverter is able to control both the magnitude and the angle of the AC output. A basic six switch three phase configuration is chosen because it is simple and well documented. The topology consists of six switches arranged in three parallel branches, where each branch has two switches in series. The switches, which are used to chop the DC voltage, are chosen to be Insulated-Gate Bipolar Transistors (IGBTs) [12]. The described inverter is shown in Fig. 7.

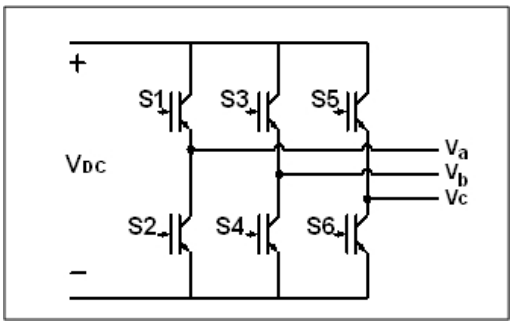

Fig. 7.Three Phase Inverter model.

G. The Inverter controller model

The proposed control system uses two PI controllers.The first PI controller controls the active power (P) of PV by adjusting the DC bus voltage between the DC-DC converter and the inverter based on [13];

$$V_{DC} \geq 1.633 V_{L-L} \qquad (14)$$

Where V_{DC} represents the dc link voltage and V_{L-L} represents the line-line voltage at the inverter side. The active power control model is shown in Fig. 8.

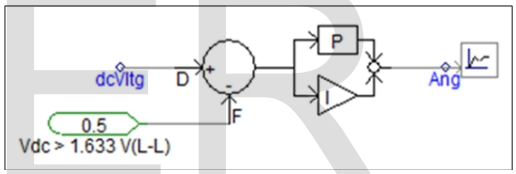

Fig. 8.The active power control model inPSCAD.

The second PI controller controls the reactive powerto either zero or inject appropriate value of reactive power (Q) from the dc link capacitor, as the PV solar system is only an active power source [13]. The reactive power control model is shown in Fig. 9.

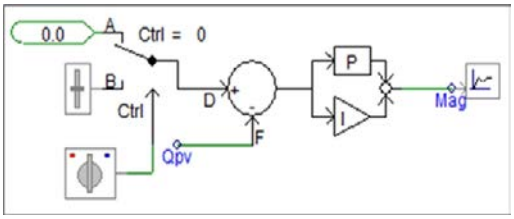

Fig. 9.The reactive power control model in PSCAD.

Controllers output of the angle and magnitude will be also used as an input tothe firing pulse generator of the inverter using PWM control technique. The firing pulse generator model is shown in Fig. 10.

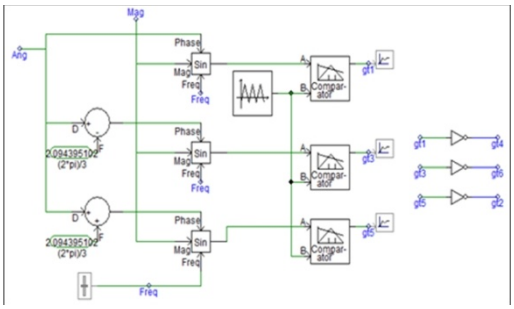

Fig. 10.The firing pulse generator model inPSCAD.

H. AC Filter Model

The filter is used to remove the high order harmonics from the voltage and current of the PV array. In this paper, LCL filter is designed based on [14] as shown in Fig.11. The size of the capacitor filter C_f is determined as follows;

$$C_f = 0.05\ C_b \qquad (15)$$

C_b is the base capacitance, it is determined as follows;

$$C_b = \frac{1}{2\pi f Z_b} \qquad (16)$$

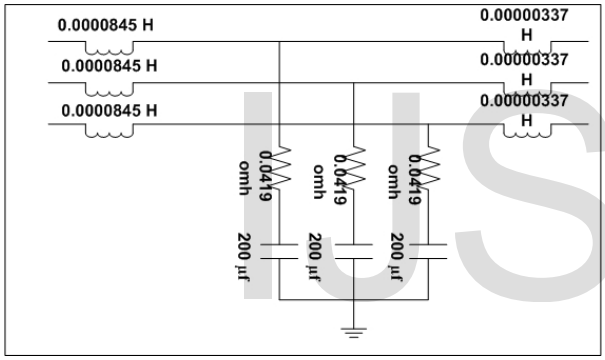

Fig. 11. LCL filter model.

f is the grid frequence, Z_b is the base impedance, is determine as follows;

$$Z_b = \frac{V_{L-L}{}^2}{p_n} \qquad (17)$$

V_{L-L} line to line voltage of inverter output and p_n is rated active power.

The size of the inverter side inductor L_1 is determined as follows;

$$L_1 = V_{dc}/6F_{sw}\Delta I_{Lmax} \qquad (18)$$

F_{sw} is PWM carrier frequency and ΔI_{Lmax} is ripple of the rated current.

$$\Delta I_{Lmax} = 10\%\ I_{max} \qquad (19)$$

$$I_{max} = p_n \sqrt{2}/3V_{ph} \qquad (20)$$

I_{max} is the rated current of inverter and V_{ph} is a phase voltage of inverter output.

The size of the grid side inductor L_2 is determined as follows;

$$L_2 = \frac{\sqrt{\frac{1}{(Ka^2)}}+1}{C_f W_{sw}{}^2} \qquad (21)$$

Ka is desired attenuation and $W_{sw} = 2\pi f_{sw}$.

The resonant frequency s determined as follows;

$$W_{sw} = \sqrt{\frac{L_1 + L_2}{L_1 L_2 C_f}} \qquad (22)$$

Finally size of the R_f is determined as follows;

$$R_f = \frac{1}{3C_f W_{sw}} \qquad (23)$$

The important conditions that should be taken into consideration at filter design are;

1. The maximum reactive power that it can absorb by the filter capacitor should be less than 5% of the rated active power to avoid lower power factor.
2. The range of the resonant frequency F_{res} should be between ten grid frequency and half of the switching frequency.
3. The summation value of the inverter side inductor and grid side inductor should be around 0.1 pu to decrease the AC voltage drop during operation.

For the model used in this paper, using 10% allowed ripple,PWM carrier frequency $f_{sw} = 15$ kHz, V_{dc}=500 V and the desired attenuation K_a= 20%. The filter capacitance is 200 µF.The inverter's and grid's inductance are calculated as 0.0845 mH and 0.00337 mH, respectively. The resonant frequency is found to be 6.251kHz. The value of damping resistance R_f = 0.0419 Ω. The produced AC voltage and current with and without filter are shown in Fig. 12.

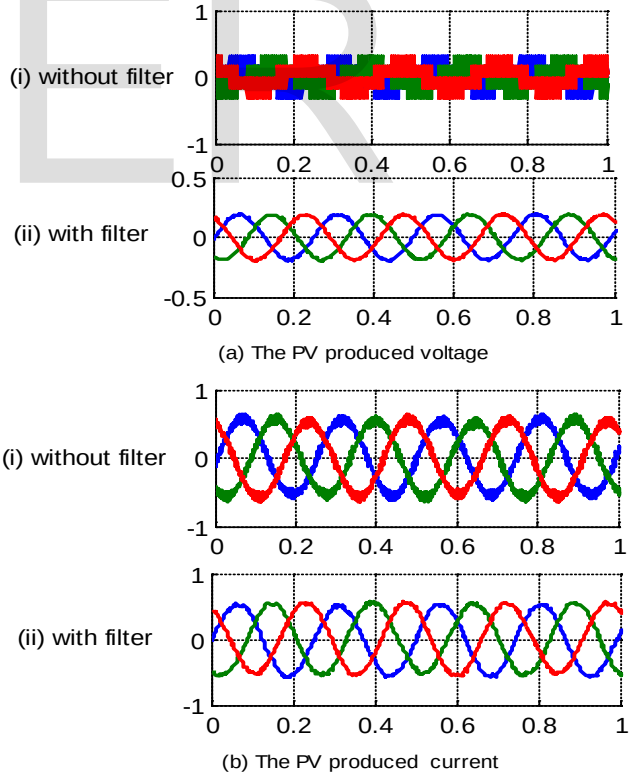

Fig. 12.The Produced AC Voltage and Current without and with filter.

I. The Coupling Transformer

A step up transformer is used as galvanic isolation between the inverter and the grid. The connection type of the step up transformer is either ungrounded wye winding, or delta winding at the inverter side therefore, when any line to ground fault occur at the AC side of the inverter, the zero sequence current through the valves are prevented to protect the IGBT valves. Ungrounded wye winding connection is used at the inverter side in order to prevent zero sequence current flow to inverter circuit and also allow zero current to flow through star earthed connection at grid side in order to make the grid protection system has the ability to detect ground faults [15].

3. VALIDATION OF THE PROPOSED CONTROLLER

The system is tested with different load values to evaluate the power factor correction capability of the PV at the PCC point. A detailed discussion about the expected range of PV cell and PV array parameters are given in Table 1 and Table 2.

Also, Fig. 13 shows the output active power from the PV panel without and with MPPT operation.

Table 1 PV Cell Parameters [2]

1	Effective area / cell (m2)	0.01
2	Series resistance / cell (Ω)	0.02
3	Shunt resistance / cell (Ω)	1000
4	Diode ideality factor	1.5
5	Band gap energy (eV)	1.013
6	Saturation current at reference conditions / cell (A)	1e-9
7	Short circuit current at reference conditions / cell (A)	2.5
8	Temperature coefficient of photo current (A/K)	0.001

Table 2 PV Array Parameters [2]

1	No. of modules connected in series / array	20
2	No. of module strings in parallel / array	20
3	No. of cells connected in series / module	108
4	No. of cell strings in parallel / module	4
5	Reference irradiation(W/m^2)	607.407
6	Reference cell temperature (c°)	50

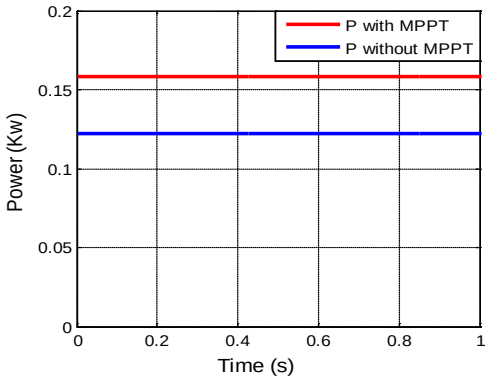

Fig. 13.The output active power of the PV panel without and with MPPT

Case 1:

It can be seen from Fig. 14 that for a load of 0.3+ j0.2 MVA (0.525 lagging power factor) the PCC current waveform before PFC lags by 58.33° the voltage waveform. Whereas, after PFC the PCC current waveform coincides with the voltage waveform. This test case shows that before power factor correction a reactive power of 0.2 MVAr will be absorbed from the grid which makes a lag power factor at the PCC to be 0.525 from the grid point of view. Whereas, for power factor correction, the needed load reactive power will be supplied from the PV. So only the active power will be absorbed from the grid and the power factor in this case is improved to 0.997 lag.

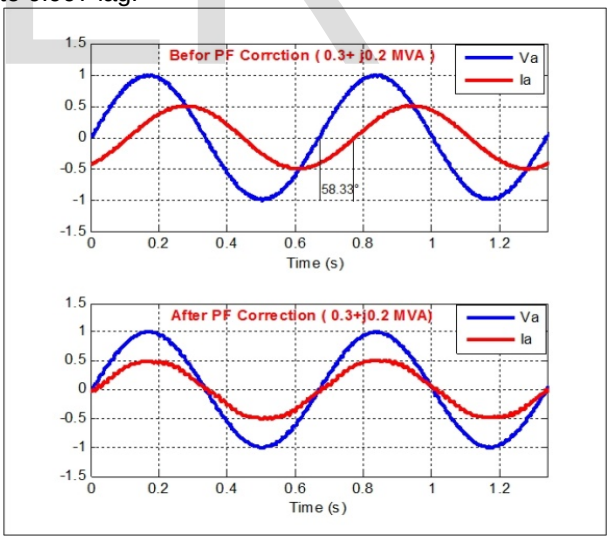

Fig. 14.Test case of (0.3+j0.2MVA)load before and after power factor correction

Case 2:

It can be seen from Fig. 15 that for a load of 0.1+ j0.1 MVA (0.447 lagging power factor) the PCC current waveform before PFC lags by 63.44° the voltage waveform. Whereas, after PFC the PCC current waveform coincides with the voltage waveform. This test case shows that before power

factor correction a reactive power of 0.1 MVAr will be absorbed from the grid which makes a lag power factor at the PCC to be 0.447 from the grid point of view. Whereas, for power factor correction, the needed load reactive power will be supplied from the PV. So only the active power will be absorbed from the grid and the power factor in this case is improved to 0.998 lag.

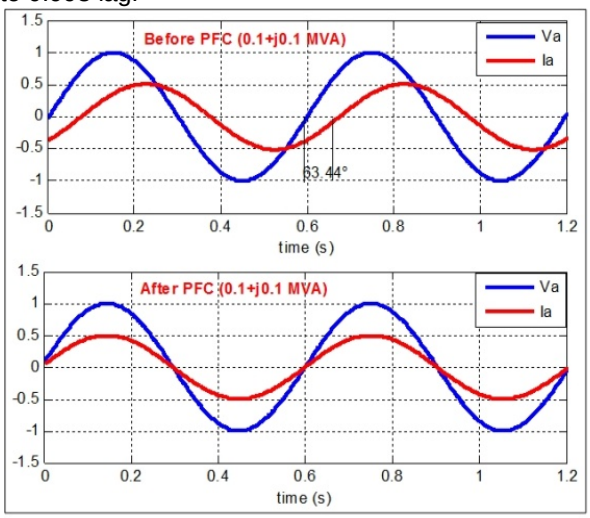

Fig. 15.Test case of load 0.1+j0.1MVA before and after power factor correction

Case 3:

It can be seen from Fig. 16 that for a load of 0.225+ j0.17 MVA (0.34 lagging power factor) the PCC current waveform before PFC lags by 70° the voltage waveform. The power factor in this case is improved to 0.998 lag.

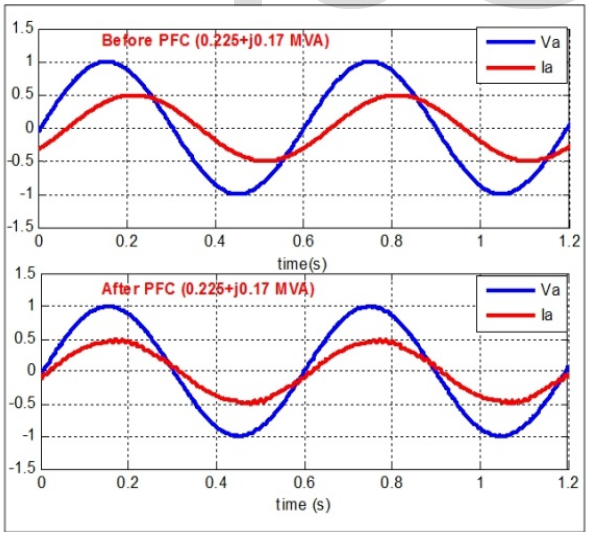

Fig. 16.Test case of (0.225+j0.17MVA)load before and after power factor correction

Case 4:

It can be seen from Fig. 17 that for a load of 0.075+ j0.05 MVA (0.78 lagging power factor) the PCC current waveform before PFC lags by 38.74° the voltage waveform. The power factor in this case is improved to 0.999 lag.

Table 3 show the active and reactive power and power factor of the grid for both before and after power factor correction for all the above test cases.

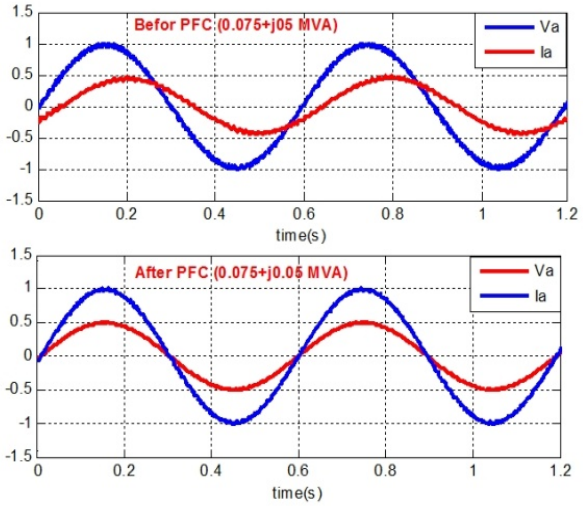

Fig. 17.Test case of (0.075+j0.051MVA)load before and after power factor correction

Table 3 Comparison between active and reactive power and power factor of the grid for all test cases.

case		1	2	3	4
Load (KW+KVAr)		300+200 J	100+100 J	225+170 J	75+50 J
Before PFC	Grid (KW+KVAr)	-135-217 j	56-112 j	-65-178 j	79.8-64 j
	PF	0.525	0.447	0.34	0.78
After PFC	Grid (KW+KVAr)	-146-115 j	54+3 j	-723-4 j	796+0.134 j
	PF	0.997	0.998	0.998	0.999

IV. CONCLUSION

In this paper, a proposed control design of grid connected PV systems for power factor correction in distribution power systems is presented. The proposed control enables the PV system act as a reactive power compensator during low radiation and day night. This helps the grid to maintain voltage stability during high reactive power loads. Also, the PV system can supply the load reactive power during high radiation and day morning. This decrease the active power due to the maximum inverter current limits. The proposed system is tested under different test cases. It is found that the PV system with the proposed control system has the capability of power factor correction.

References

[1] EPIA - European Photovoltaic Industry Association "Global Market Outlook for Photovoltaic 2014-2018", 12 June 2014, Available at http://www.epia.org.

[2]Anthony W. Ma, "Modeling and Analysis of a Photovoltaic System with a Distributed Energy Storage System," San Luis Obispo, M.Sc. Thesis, 2012.

[3] K. K. Weng, W.Y. Wan, and R. K. Rajkumar, "Power Quality Analysis for PV Grid Connected System Using PSCAD/EMTDC", International Journal of Renewable Energy Research (IJRER), Vol. 5, No. 1, 2015, pp.121-132.

[4] AdedamolaOmole, "Voltage Stability Impact of Grid-Tied Photovoltaic Systems Utilizing Dynamic Reactive Power Control", South Florida. Ph.D. Thesis, 2010.

[5] K.Chatterjee, B. G. Fernandes, and G. K. Dubey, "An Instantaneous Reactive Volt-Ampere Compensator and Harmonic Suppressor System", IEEE Transactions on Power Electronics, Vol. 14, No. 2, 1999, pp.381-392.

[6] S. Malki, "Maximum Power Point Tracking (MPPT) for Photovoltaic System", M.Sc. Thesis, 2011.

[7] A.Preethi, and S. Devi Vidhya. "An Approach To Achieve Maximum Power Point Tracking Using PV System For Buck Converter." IJSER , Vol. 5, No. 4, 2014, pp. 89-95.

[8] R.Faranda and S. Leva, "Energy Comparison of MPPT Techniques for PV Systems", WSEAS Transactions on Power Systems , Vol. 3, No. 6, 2008, pp. 446-455.

[9] A Tariq, M. Asim, and M. Tariq. "Simulink Based Modeling, Simulation and Performance Evaluation of an MPPT for Maximum Power Generation on Resistive Load", 2nd International Conference on Environmental Science and Technology, Vol. 6, 2011.

[10]A. Jusoh, "A Review on Favorable Maximum Power Point Tracking Systems in Solar Energy Application", TELKOMNIKA (Telecommunication Computing Electronics and Control), Vol. 12, No. 1, 2014, pp. 6-22.

[11] A.Kalbat, "PSCAD Simulation of Grid-Tied Photovoltaic Systems and Total Harmonic Distortion Analysis",3rd International Conference on Electric Power and Energy Conversion Systems (EPECS), Oct 2013, pp.1-6.

[12] B. A. Johnson, "Modelling and Analysis of a PV Grid-Tied Smart Inverter's Support Function," San Luis Obispo, M.Sc. Thesis, 2013.

[13] B. Das, "Novel Control and Harmonics Impact of PV Solar Farms", Western University London, M.Sc. Thesis, 2012.

[14] B.Liu and B. Song, "Modeling and Analysis of an LCL Filter for Grid-Connected Inverters in Wind Power Generation Systems." IEEE Power and Energy Society General Meeting, 2011, pp. 1-6.

[15] "Operation and Maintenance Manual for 10kW Grid-Tied Photovoltaic Inverter", Trace Technologies, 1999.